JOURNAL OF PHYSIOLOGY AND PHARMACOLOGY 2015, 66, 2, 273-283
www.jpp.krakow.pl

T. GWAG[1], K. PARK[2], J. PARK[1], J.-H. LEE[3], T. NIKAWA[4], I. CHOI[1]

CELASTROL OVERCOMES *HSP72* GENE SILENCING-MEDIATED MUSCLE ATROPHY AND INDUCES MYOFIBER PRESERVATION

[1]Division of Biological Science and Technology, College of Science and Technology, Yonsei University, Wonju, Gangwon-Do, Republic of Korea; [2]Sungkyunkwan University, Medical Research Institute, Clinical Research Center, Samsung Biomedical Research Center, Seoul, Republic of Korea; [3]Korea Aerospace Research Institute, Yuseong-gu, Daejeon, Republic of Korea; [4]Department of Nutritional Physiology, Institute of Health Biosciences, University of Tokushima Graduate School, Tokushima, Japan

To elucidate a potential anabolic role of heat shock proteins (HSPs) in myofiber preservation, we assessed the effect of *HSP70* gene silencing versus its overexpression on skeletal muscle atrophy or rescue. *HSP72* gene expression was silenced by pre-treatment with *HSP72* siRNA in cultured rat L6 myotubes, and the pro-anabolic effect of HSPs was examined in the absence or presence of the HSP inducer celastrol (CEL). Compared to the negative control (NC), both nuclear accumulation and phosphorylation of heat shock transcription factor 1 remained high under the 6-h treatment of CEL. The *HSP72* siRNA treatment significantly decreased *HSP72* mRNA and protein expression and myotube diameter. CEL treatment, however, markedly increased the HSP72 expression and rendered the myotube size recovered to the NC level even in the siRNA-treated cells. Moreover, the *HSP72* siRNA upregulated forkhead box O3 (FoxO3) expression in the nucleus while CEL increased *p*-FoxO3 exclusively in the cytoplasm, thus leaving the *p*-FoxO3/FoxO3 balanced to the NC level by siRNA + CEL treatment. The atrophic effect of *HSP72* siRNA was consistent with the upregulation of atrogin-1 and proteasome activity but CEL treatment abrogated such effect by activation of Akt1, ribosomal S6 kinase (S6K) and extracellular signal-regulated kinase 1/2 (ERK1/2), irrespective of *HSP72* silencing. These results suggest that CEL-mediated overexpression of HSP72 overcomes the atrophic effect of HSP72 gene silencing *via* both enhancement of FoxO3 phosphorylation and activation of Akt1-ERK1/2 signaling pathway.

Key words: *heat shock protein 72, celastrol, extracellular signal-regulated kinase 1/2, forkhead box O3, gene silencing, proteasome, ubiquitin E3 ligase, muscle-specific RING finger-1*

INTRODUCTION

An anabolic role of heat shock proteins (HSPs) in myofiber preservation has been a central issue in rehabilitation and space medicine (1, 2). HSPs are known to act as molecular chaperones for protein expression and quality control under variable stresses (3-5). For instance, disuse atrophy of skeletal muscle has been associated with downregulation of HSP70 expression and is ameliorated when HSP70 is overexpressed by heat stress. This anti-atrophic effect of HSP70 was found to be linked to the concurrent activities of several signaling pathways: (i) the activation of anabolic routes including Akt/protein kinase B, mammalian target of rapamycin (mTOR) to ribosomal S6 kinase (S6K), and mitogen-activated protein kinase/extracellular signal-regulated kinase 1/2 (MAPK/ERK1/2) and (ii) suppression of the catabolic axis involving ubiquitin E3 ligases, such as atrogin-1 and muscle-specific RING finger-1 (MuRF1), to proteasomes (1, 6).

It has also been demonstrated that overexpression of HSP70 inhibits muscle atrophy by suppressing nuclear factor kappa-light-chain-enhancer of activated B cells (NF-κB) and FoxO3 transcriptional activities that otherwise increase E3 ligase expression (2, 7). Recently, pharmaceutical application intended to induce HSP overexpression has been attempted, which addresses the suppressive effect of HSP on catabolic signals including FoxO3 and E3 ligase (1, 6). For example, the *in vivo* treatment of 17-allylamino-17-demethoxygeldanamycin (17-AAG) attenuated the atrophy of the unloaded rat soleus muscle that accompanies increases in *HSP70* and *HSP90* mRNA levels, retention of *p*-FoxO3 and suppression of ubiquitin, atrogin-1 and μ-calpain contents (1). This accumulating evidence suggests that HSPs, particularly HSP70, are potent chaperones that assist in muscle mass retention, even in atrophy-inducing conditions. However, to validate a regulatory function of HSP70 for muscle mass growth, it is necessary to determine whether active suppression of HSP70 directly causes muscle atrophy and if HSP70 overexpression counteracts the atrophy *via* differential modulation of anabolic and catabolic signals. This question remains to be addressed.

The heat shock response (HSR) is a highly conserved cytoprotective mechanism and is known to exist in all organisms from yeast to humans (8, 9). In an unstressed condition, heat shock

transcription factor 1 (HSF1) stays in the cytoplasm as a monomeric form in a complex with HSP40, HSP70 and HSP90. Under stressful conditions, the HSF1 is separated from the HSP complex and forms trimeric HSF1, which is then translocated into the nucleus and binds to the heat shock element of the target gene (8, 9). The transactivation of HSF1 occurs with its phosphorylation at Ser230, which is most likely regulated by calcium/calmodulin-dependent protein kinase II (CaMKII) (10, 11).

In prior studies, we and others showed that HSP70 overexpression was induced by treatment with celastrol (CEL), a natural compound derived from *Tripterygium wilfordii Hook*, to various cell lines including HeLa, SH-SY5Y and mouse C2C12 myotubes (6, 12, 13). This HSP70 inducer was found to activate the hsp70.1 promoter, and its HSR kinetics was similar to those incurred by heat stress (13). Our recent study further showed that CEL-treated C2C12 myotubes had an increased cell diameter of 13% and an elevated nuclear accumulation of *p*-HSF1 and HSP72 expression compared to control cells (6). Moreover, the CEL treatment completely abolished dexamethasone-induced atrophy of the myotubes by the activation of anabolic signaling proteins (Akt1-ERK1/2) and a suppression of catabolic signaling proteins (FoxO3, MuRF1 and proteasome activity).

In this study, we explored our fundamental question of the chaperone function of HSPs in cell size preservation. For this goal, we investigated whether the silencing of the *HSP70* gene led to muscle atrophy with changes in the aforementioned signaling responses and whether such atrophy was abrogated by overexpression of HSP70 *via* treatment with the HSP inducer. We silenced *HSP70* gene expression by pre-treatment with *HSP72* siRNA in cultured rat L6 myotubes and determined the myotube diameter, HSF1 and *HSP72* expression, and assayed the anabolic and catabolic signaling activities in the presence or absence of CEL. Our findings demonstrated that gene silencing markedly reduced the expression of the *HSP72* gene and its protein and led to significant myotube atrophy with inhibition of signaling molecules involved in muscle growth, whereas these atrophic effects were completely counteracted by *HSP72* overexpression.

MATERIAL AND METHODS

Reagents and stock solutions

CEL (Cayman Chemical, Ann Arbor, MI, USA) was dissolved in dimethyl sulfoxide (DMSO; Sigma-Aldrich, St. Louis, MO, USA) at a stock concentration of 25 mM. Dulbecco's modified Eagle's medium (DMEM) was purchased from Welgene (Dalseogu, Daegu, Korea). Fetal bovine serum (FBS) was purchased from Hyclone (Logan, UT, USA). OPTi-MEM, an antibiotic-antimycotic, was purchased from Gibco (Burlington, Ontario, Canada). *HSP72* siRNAs were purchased from ST Pharm (Gangnam-gu, Seoul, Korea). Lipofectamine RNAiMAX was purchased from Invitrogen (Grand Island, NY, USA). Nonidet P-40, the Complete Mini protease inhibitor, and a phosphatase inhibitor cocktail were purchased from Roche (Mannheim, Germany). Restore™ Western blot stripping buffer was purchased from Thermo Scientific (Rockford, IL, USA). A mouse anti-HSP72 monoclonal antibody was purchased from Stressgen (Victoria, BC, Canada); rabbit anti-Akt1, phospho-Akt1 (at Ser^{473}), FoxO3, phospho-FoxO3 (at Ser^{256}), ERK1/2, and phospho-ERK1/2 (Thr202/Tyr204) polyclonal antibodies were purchased from Cell Signaling Technology (Beverly, CA, USA); a rabbit anti-MuRF1 polyclonal antibody was purchased from ECM Biosciences (Versailles, KY, USA); a mouse monoclonal antibody to glyceraldehydes-3-phosphate dehydrogenase (GAPDH) and a rabbit polyclonal antibody to MAFbx were purchased from Abcam (Cambridge, UK); and an HRP-conjugated anti-mouse IgG, anti-rabbit IgG and Alexa Fluor 488 goat anti-rabbit IgG were purchased from Cell Signaling Technology.

Cell culture

Rat L6 myoblastic cells were procured from the American Type Culture Collection (Rockville, MD, USA) and were grown in growth medium (10% FBS and 1% antibiotic-antimycotic in DMEM). When the myoblasts were approximately 80–90% confluent, the cells were differentiated into myotubes *via* incubation in differentiation medium (2% FBS and 1% antibiotic-antimycotic in DMEM) for 7 d. The cells were maintained at 37°C under 5% CO_2, and the medium was changed every other day.

HSP72 siRNA transfection

After 7 days of differentiation, three groups of L6 myotubes were transfected with either universal negative control siRNA (hereafter called 'NC') or two *HSP72* siRNAs [siRNA1 and siRNA2]. The sequence of siRNAs is described in *Table 1*. A total of 250 nM siRNA in opti-MEM was combined with lipofectamine RNAiMAX in opti-MEM. The mixture was incubated for 20 min at room temperature and added to cells in 4% FBS and antibiotic/antimycotic-free DMEM resulting in a final concentration of 2% FBS. After 24 hours, the cell medium was replaced with 2% FBS and antibiotic/antimycotic-free DMEM. The cells were incubated for 48 hours in a CO_2 incubator for the *HSP72* gene silencing experiments. The efficiency of the two *HSP72* siRNAs was tested by comparing protein expression levels of HSP72 and FoxO3 by immunoblotting analysis. From this analysis, the siRNA2 ('siRNA') was chosen for subsequent assays (see Results). After the siRNA transfection, 2.0 μM of CEL was added to L6 cells labeled as NC + CEL and siRNA + CEL, and then cells were incubated for an additional 6 hours. Because CEL was dissolved in the DMSO solution, the same volume of DMSO was also added to both the NC and siRNA-treated cells.

Immunofluorescence staining and confocal microscopy

The L6 cells were maintained on cover glass-bottom dishes (SPL, Pocheon-si, Gyeonggi-Do, Korea) during growth, differentiation, siRNA transfection and CEL treatment. The cells were washed three times with 1X PBS and fixed in 4% paraformaldehyde for 30 min at room temperature. The cells were permeabilized with 0.2% Triton X-100 for 25 min on ice and blocked with 3% BSA in 1X PBS. The cells were stained with primary antibodies (1:100) to HSF1 and FoxO3 in 1X PBS and allowed to react with Alexa 488-rabbit secondary antibody (1:1,000). The cells were washed three times with 1X PBS, and then mounted with a mounting medium with DAPI (Vector Laboratories, Burlingame, CA, USA). The fluorescently labeled cells were observed with a Carl Zeiss LSM710 confocal microscope (Jena, Germany). Finally, to assess the effect of siRNA and CEL treatments on subcellular localization of HSF1, the nuclear fluorescence intensity of the HSF1 was analyzed for the confocal images using the Image J software (NIH, Frederick, MD, USA).

Real-time quantitative PCR

Total RNA from each cell group was extracted using TRIzol (Invitrogen Life Technology, Carlsbad, CA, USA) according to

Table 1. Summary of primer and siRNA sequence.

Gene Name	Sequences (5' → 3')		GenBank Accession No.
real-time PCR primer		Product size (bp)	
Hsp72	F: CAAGATCACCATCACCAACG R: GCTGATCTTGCCCTTGAGAC	193	NM_031971
GAPDH	F: GTGACTTCAACAGCAACTCCCATTC R: GTGGTCCAGGGTTTCTTACTCCTTG	173	NM_017008
siRNA sequence			
Negative Control	F: AUGAACGUGAAUUGCUCAA R: UUGAGCAAUUCACGUUCAU		
HSP72 (1)	F: GCGAGAACCGGUCGUUCUA R: UAGAACGACCGGUUCUCGC		NM_031971
HSP72 (2)	F: GCGACCUGAACAAGAGCVA R: UGCUCUUGUUCAGGUCGC		NM_031971

the manufacturer's protocol. RNA concentrations were measured with a spectrophotometer (Biorad, Hercules, CA, USA). Total RNA was treated with RQ1 RNase-Free DNase (Promega, Madison, WI, USA) and then used to synthesize cDNA with ImProm-II Reverse transcriptase (Promega). Real-time quantitative PCR (qPCR) was performed using a Power SYBR Green PCR Master Mix (Applied Biosystems, Foster City, CA, USA) on an Applied Biosystems StepOnePlus System (Applied Biosystems) using the following procedure: one cycle of 95°C for 10 min and 40 cycles of 95°C for 30 s, 60°C for 30 s, and 72°C for 30 s. Melting curve data confirmed the specificity of the primer (see *Table 1* for primer sequences) and single product amplification. The results were normalized to those of GAPDH, which was used as an internal control. The cycle number at which the reaction crossed an arbitrary threshold (CT) was determined for each gene and analyzed using the $2^{-\Delta\Delta Ct}$ method.

Cell size determination

To determine the effects of *HSP72* siRNA and CEL on L6 myotube size, cells from each group were photographed at 100× magnification under a phase-contrast microscope after fixation with 4% paraformaldehyde. The fields were divided into 16 compartments to randomly select cells for the analysis. The diameters of individual myotubes were measured using the Image J software (NIH, USA).

Cell fractionation

L6 cells were washed, harvested with 1X PBS and centrifuged for 5 min at 3,000 rpm at 4°C. The cell pellet was washed with hypotonic buffer (10 mM Tris-HCl (pH 7.5), 10 mM NaCl, 1 mM KH_2PO_4, 1 mM $CaCl_2$, 0.5 mM $MgCl_2$, 5 mM $NaHCO_3$, protease inhibitor cocktail and phosphatase inhibitor cocktail) and was suspended in 500 µl of hypotonic buffer. After 10 min of incubation on ice, the swollen cells were homogenized 50 times with a Dounce homogenizer and centrifuged for 10 min at 7,500 rpm at 4°C. The supernatant was transferred into a new microtube to harvest cytoplasm proteins, and the pellet was homogenized in cell lysis buffer (50 mM HEPES [pH 7.4], 150 mM NaCl, 2 mM EDTA, 1% Nonidet P-40, 20 mM β-glycerophosphate, 0.2 mM Na_3VO_4, 50 mM NaF, the protease inhibitor Complete Mini and a phosphatase inhibitor cocktail) *via* sonication, then the lysate was centrifuged at 13,000 rpm for 15 min at 4°C, and the supernatant was retained as the nuclear fraction.

Immunoblotting analysis

The protein concentration of each of whole lysate, cytoplasm and nucleus was determined with a Bradford assay. A total of 30-50 µg of protein was subjected to SDS-PAGE on 8-12% gels as indicated to detect HSP72, Akt1, phospho-Akt1 (*p*-Akt1), FoxO3, *p*-FoxO3, MuRF1, atrogin-1, ERK1/2 and *p*-ERK1/2. The proteins were electrophoretically transferred from the gel to a nitrocellulose membrane. The membrane was incubated in blocking buffer (1 × TBS, 0.5% Tween-20 with 5% w/v nonfat dry milk) at room temperature for 1 hour and was washed with 10 ml TBS/T three times for 5 min each. The membrane was subsequently incubated at 4°C overnight with the corresponding primary antibody at the indicated dilution (1:500-1:10,000) in 10 ml of primary antibody dilution buffer. The membrane was then incubated with an HRP-conjugated secondary antibody (1:1,000-1:20,000) in 10 ml of blocking buffer under gentle agitation at room temperature for 1 hour to detect bound proteins and was washed three times for 5 min each with 10 ml of TBS/T between incubations. Immune complexes were detected with an ECL system (GE Healthcare, Fairfield, CT, USA), and the obtained bands were quantified using a densitometer (Bio-Rad). The densities of the proteins were normalized to that of GAPDH. The membranes were stripped off using the Restore buffer (15 ml/membrane) and then used to detect the second protein by incubation with the corresponding antibody.

26S proteasome activity assay

The four groups of myotubes were trypsinized and washed with fresh differentiation medium. Among the three determinants of proteasome activity (i.e., trypsin-, chymotrypsin- and caspase-like activities), chymotrypsin-like activity was measured and considered to be representative of the proteolytic capacity of the proteasome. Using approximately 7.5 × 10^3 cells, as counted with a cell counter (Biorad, Hercules, CA, USA), in 50 µl of differentiation medium, chymotrypsin-like activity was determined using the Promega Proteasome-Glo™ cell based luminescent assay kit (Promega, Madison, WI, USA) according to the manufacturer's protocol. To confirm the specificity of the assay, an aliquot containing the same number

of cells was pretreated for 0.5 h with 10 μM epoxomicin, a proteasome inhibitor. Chymotrypsin-like activity was determined with the same procedure and the outcome was used as the background signal for this assay. Luminescence was determined with a GloMax 20/20 Luminometer (Promega).

Data analysis

All data are presented as the mean ± S.E.M. The significance of intergroup differences in the means was examined *via* one-way analysis of variance (ANOVA) and SNK *post-hoc* multiple comparison tests. Statistical analyses were performed with SPSS/PC+, and a value of $P < 0.05$ was considered statistically significant.

RESULTS

Knockdown of HSP72 by siRNA suppressed HSP72 expression and enhanced FoxO3 expression in a dose-dependent manner

To determine the efficiency of *HSP70* gene silencing, rat L6 myotubes were treated with two *HSP72* specific-siRNAs [siRNA1 and siRNA2], and the effect of silencing was

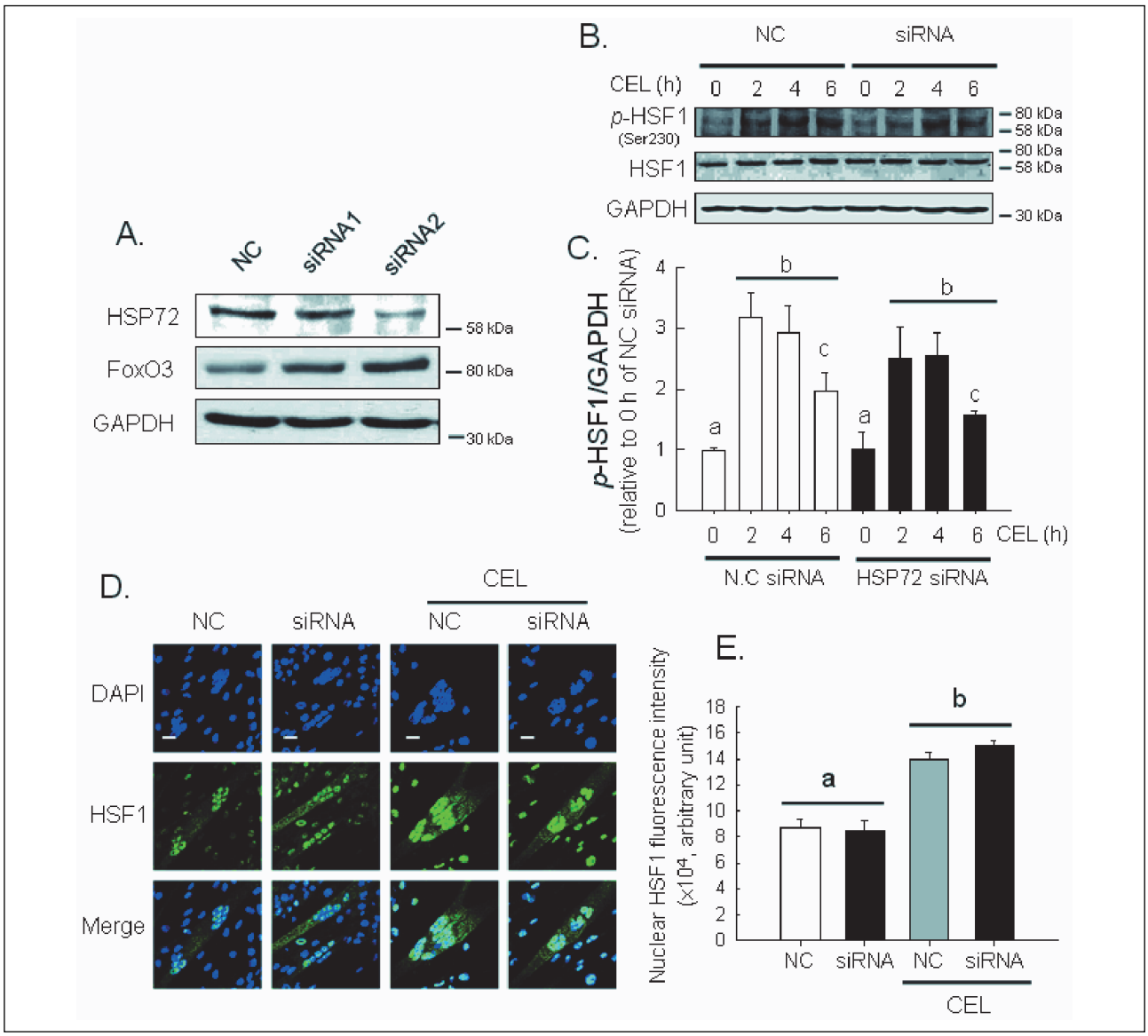

Fig. 1. (A) Effect of knockdown of *HSP72* gene on HSP72 and FoxO3 protein expression. The HSP72 and FoxO3 levels were determined by immunoblot analysis using whole-cell lysates prepared from NC, siRNA1 and siRNA2 treated rat L6 myotubes. GAPDH was used as a protein loading control. (B, C) Upregulation of *p*-HSF1 in the rat L6 cells treated with CEL for 6 hours under the HSP72-specific siRNA-mediated gene silencing. The total HSF1 remained constant for the period indicated. Whole cell lysates were subjected to immunoblot analyses with Ser^{230}-phosphorylated HSF1. Mean ±S.E.M. (n=5). The symbols a, b and c indicate statistical significance among the groups with $P < 0.05$. (D) Confocal immunofluorescence analysis to visualize the subcellular localization of HSF1 in the NC, siRNA, NC + CEL and siRNA + CEL treated groups. L6 myotubes were stained with an HSF1 antibody followed by a secondary antibody conjugated to Alexa488 (green). Nuclei were visualized by staining with DAPI (blue). White scale bars =20 μm. (E) Quantitative summary illustrating the nuclear accumulation of HSF1 with the CEL treatment. The HSF1 fluorescence intensity in the nucleus was determined using the Image J software for a total of 24 nuclei per group. Mean ± S.E.M. (n=4), a versus b, $P < 0.05$.

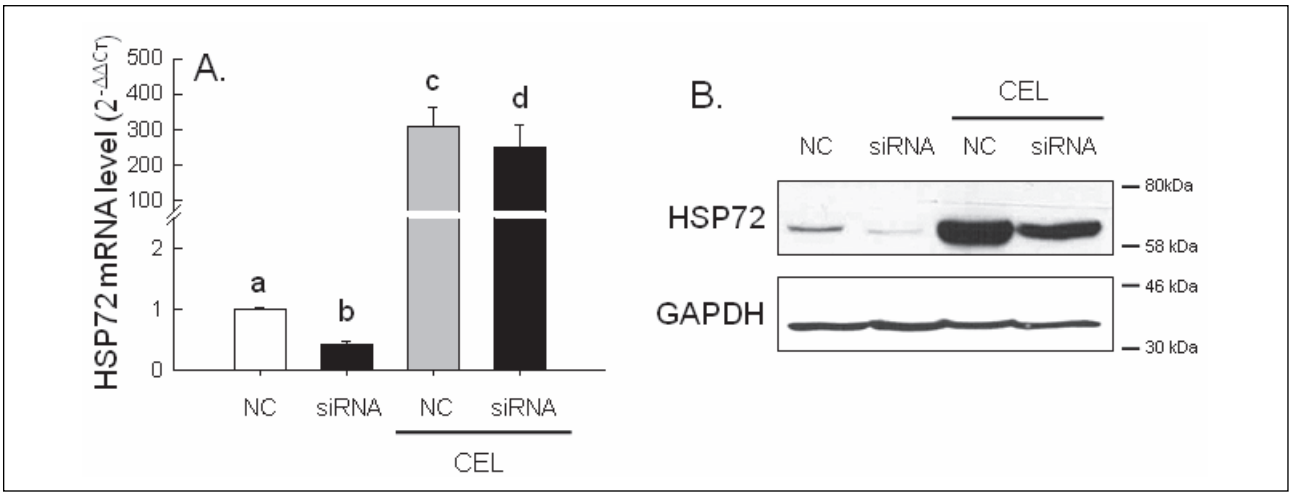

Fig. 2. Upregulation of HSP72 expression by CEL treatment in the L6 myotubes. (A) *HSP72* mRNA levels of the four groups were determined by real-time PCR. Data represent mean ±S.E.M. (n=4, each with duplicate experiments). (B) HSP72 protein expression was determined by immunoblot analysis using whole-cell lysates prepared from the four groups. GAPDH was used as a protein loading control. Data represent mean ±S.E.M. (n=6). The symbols a, b, c and d indicate statistical significance among the groups with $P < 0.05$.

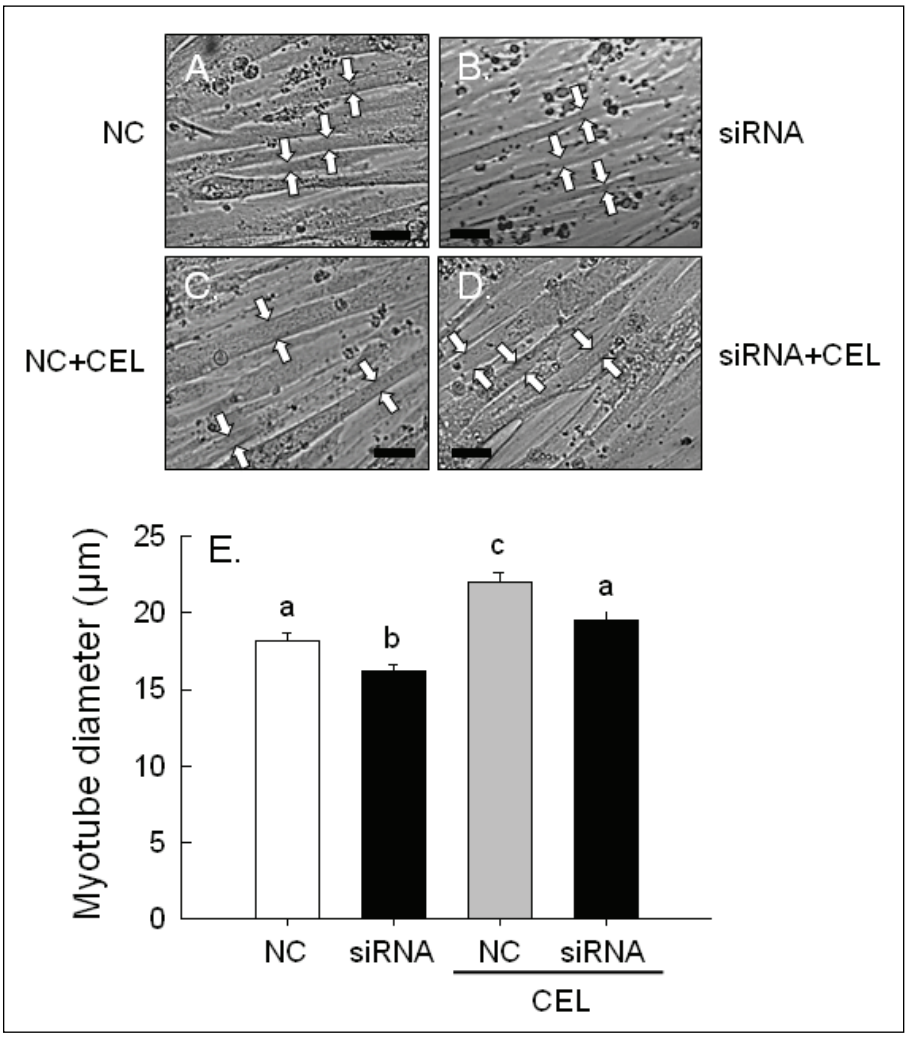

Fig. 3. (A-D) Representative photographs of L6 myotubes for the NC, siRNA, NC + CEL and siRNA + CEL groups, respectively. Black bars = 50 μm. Arrows point out the region of that myotube used for diameter measurement which was relatively slim along the cell. (E) Comparison of the myotube diameters among the four groups. Data represent mean ±S.E.M. (n=178–183 cells per group with 3 independent experiments). The symbols indicate significant differences among groups with $P < 0.05$.

determined by immunoblotting analysis. We observed different efficiencies of downregulation in *HSP72* gene expression (*Fig. 1*). Relative to the level of the universal negative control siRNA (NC), HSP72 expression was reduced and FoxO3 expression was increased by siRNA1 and siRNA2 at a concentration of 62.5 nM in a potency-dependent manner (*Fig. 1A*). Based on these

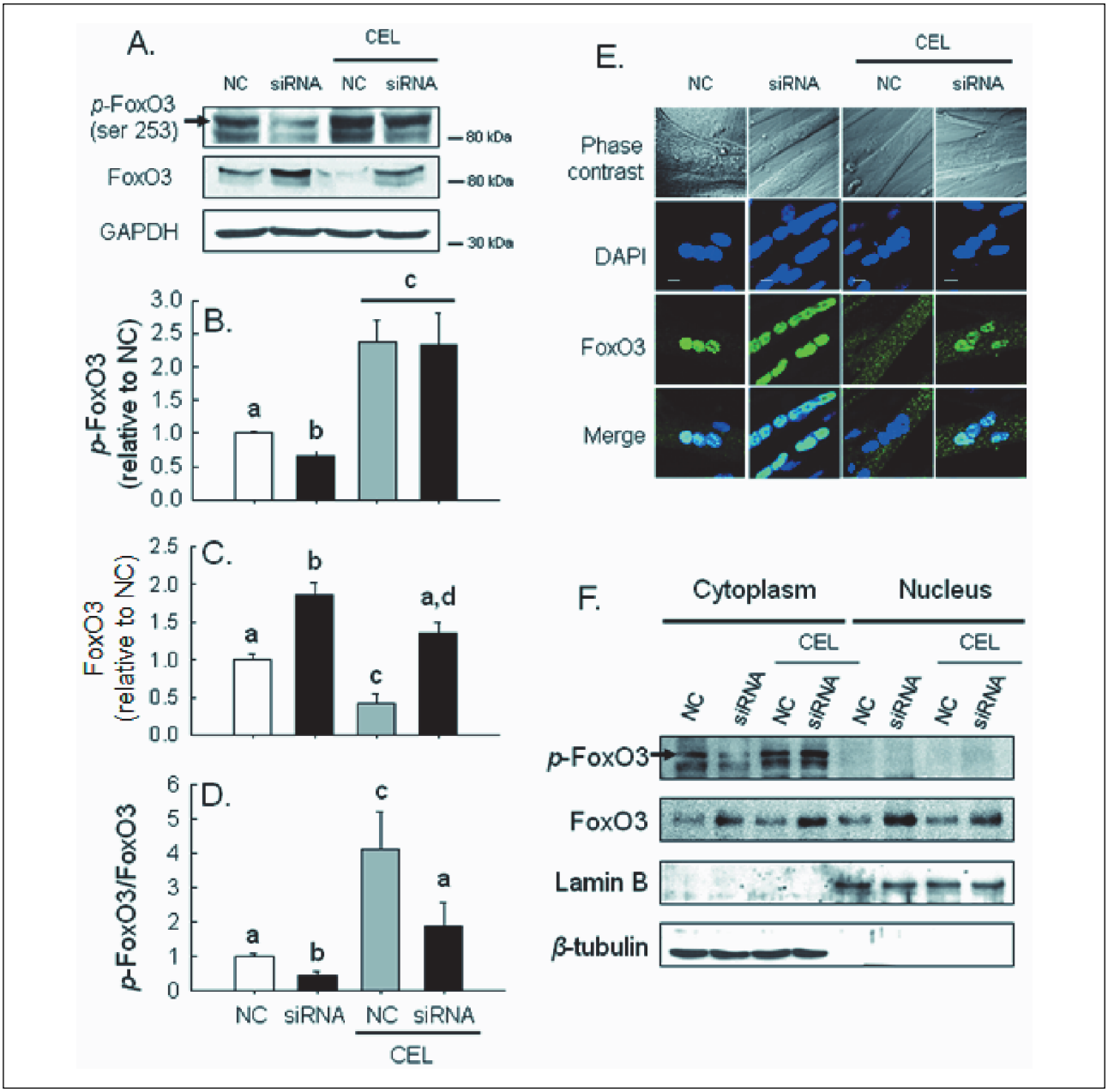

Fig. 4. Regulation of FoxO3 signaling by *HSP72* siRNA and CEL. (A) Expression of *p*-FoxO3 (Ser^{253}) and total FoxO3 were detected by immunoblot analysis using whole-cell lysates obtained from the four groups. GAPDH was used as a protein loading control. (B-D) Densitometric quantitation of *p*-FoxO3 and total FoxO3 levels. Mean ±S.E.M. (n=6). a versus b, a versus c, b versus c, and c versus d, P <0.05. (E) Confocal immunofluorescence images to visualize the subcellular localization of FoxO3. The cells were stained with a FoxO3 antibody followed by a secondary antibody conjugated to Alexa488 (green), and the nuclei were stained with DAPI (blue). White bars = 10 μm. (F) The subcellular fractionation analysis of *p*-FoxO3 and FoxO3. The proteins in the cytoplasm and nuclei were separated by hypotonic buffer and a Dounce homogenizer, and expression levels were detected by immunoblot analysis. The appropriateness of subcellular fractionation was confirmed by immunoblot analysis with anti-laminB and anti-β-tubulin as a marker for nuclear and cytoplasm fractionation, respectively.

results, *HSP72* siRNA2 was chosen for subsequent experiments [hereafter called '*HSP72* siRNA'].

Celastrol treatment led to activation and nuclear accumulation of HSF1

To address the effect of *HSP72* silencing on HSF1 activation, and whether CEL treatment rescued the *HSP72* silencing effect, L6 cells were treated with either NC or *HSP72* siRNA and then treated with CEL for 6 hours as indicated. *Fig. 1B* and *1C* illustrates the time-course change in the HSF1 expression and its phosphorylation (at Ser230) determined by immunoblotting analysis. Compared to the levels just prior to the initial treatment, *p*-HSF1 expression increased 3.2- and 2.5- fold as early as 2 hours after CEL treatment in the NC + CEL and *HSP72* siRNA + CEL groups, respectively (P <0.05). The level remained significantly increased at 6 hours after CEL treatment (P <0.05). The total HSF1 level did not change over the 6-h treatment of CEL in both NC and siRNA groups (*Fig. 1B*). To further confirm these results, we assessed the subcellular

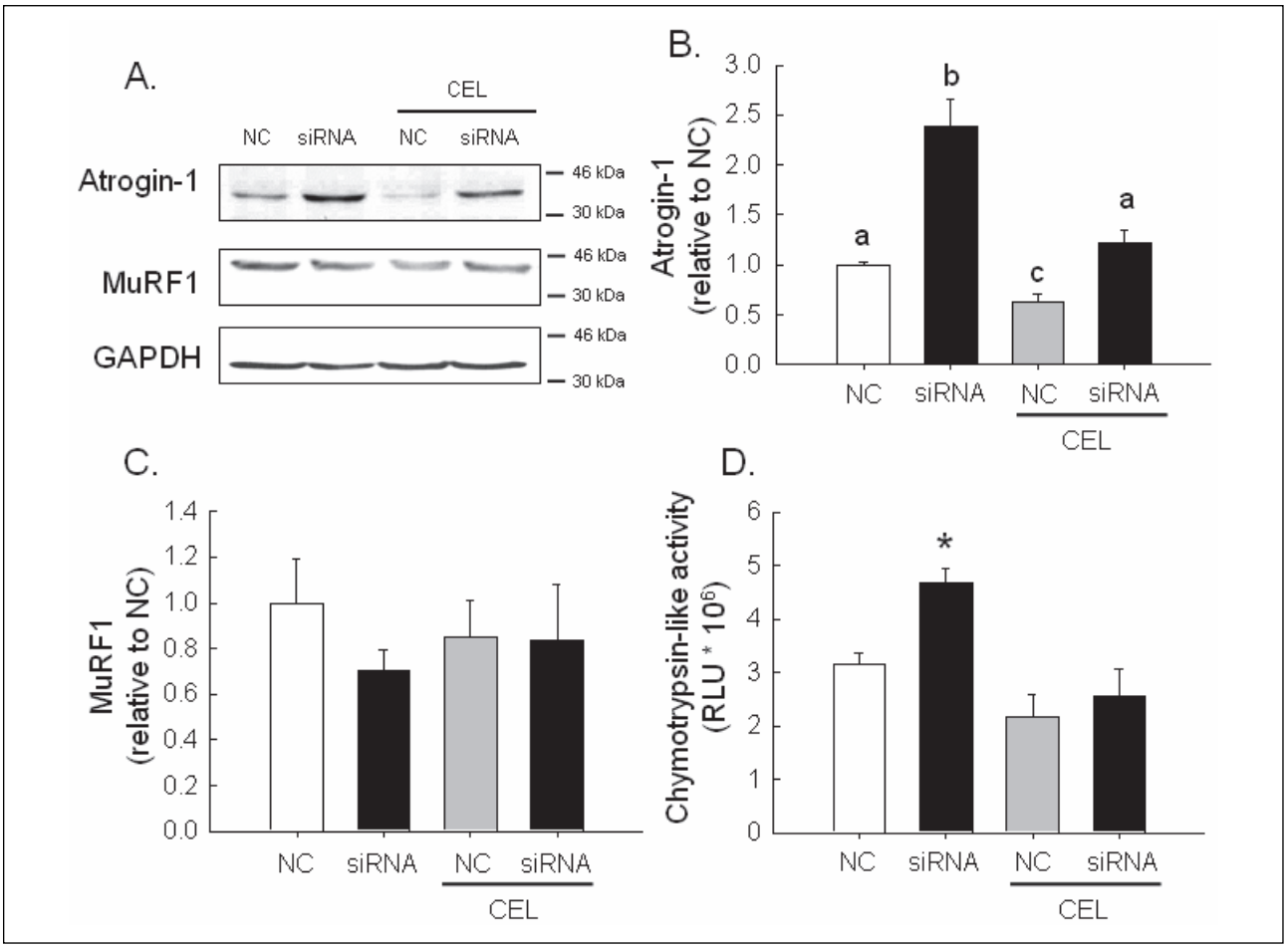

Fig. 5. Intergroup comparisons of E3 ligase expression levels and proteasome activity by HSP72 siRNA and CEL treatment. (A) Bands from immunoblot analysis and (B-C) densitometric quantitation of atrogin-1 and MuRF1 expression. Mean ± S.E.M. (n=6). P <0.05 among a, b and c. (D) The chymotrypsin-like activity of the 26S proteasome determined *via* a cell-based luminescent assay and presented in relative light units (RLU). Data were obtained from three independent experiments with each performed in duplicate. Mean ±S.E.M. (n=3). * P <0.05.

localization of HSF1 by indirect immunofluorescence staining followed by quantitation analysis of HSF1 fluorescence intensity in the nuclei of the four groups (*Fig. 1D* and *1E*). We observed considerable accumulation of HSF1 (1.8-fold) in the nuclei of the two CEL-treated groups compared to those treated with NC or *HSP72* siRNA alone (P <0.05). Taken together, these results suggest that CEL treatment led to nuclear accumulation and activation of HSF1, irrespective of *HSP72* siRNA treatment.

Celastrol treatment markedly enhanced HSP72 mRNA and protein expression, which remained increased in the presence of HSP72 siRNA

Our previous experiment revealed the marked induction of *p*-HSF1 and HSP protein by CEL treatment in C2C12 cells (6). Thus, we addressed whether siRNA-mediated *HSP72* gene silencing could be rescued by CEL treatment. Relative to the NC level, *HSP72* mRNA expression was knocked down 57% with *HSP72* siRNA (*Fig. 2A*). In contrast, CEL treatment led to dramatic increases of *HSP72* mRNA in the NC + CEL (300-fold) and siRNA + CEL (250-fold) groups. Next, we also assessed the effect of *HSP72* siRNA on its protein expression (*Fig. 2B*). The effect of *HSP72* siRNA and CEL on HSP72 protein expression showed a similar pattern to that of the mRNA expression. The HSP72 protein level was decreased 65% with *HSP72* siRNA treatment but increased 8.8- to 6.3-fold in two CEL-treated groups (quantitation not shown). The significant difference in both the mRNA and protein levels was also evident between the NC + CEL and siRNA + CEL groups.

HSP72 gene silencing induced L6 myotube atrophy, whereas celastrol treatment abrogated that effect

To demonstrate the functional significance of *HSP72* gene silencing and CEL treatment on the L6 cell size, differentiated myotubes were treated with *HSP72* siRNA and then processed with or without CEL treatment. Representative photos of individual L6 myotubes are shown in *Fig. 3A-3D*. The myotube diameter was 19.2 ± 0.58 μm in the NC group but was decreased to 84% in the *HSP72* siRNA group (P <0.05) (*Fig. 3E*). The myotube diameter, however, was increased 1.15-fold in the NC + CEL versus the NC group (P <0.05) and was retained at the size of the NC group in the siRNA + CEL treatment (19.58 ± 0.53 μm) (P >0.05).

HSP72 siRNA increased FoxO3 expression but celastrol treatment counteracted this increase

FoxO3 protein is known as an important regulator of ubiquitin E3 ligase expression in muscle atrophy (7), and our

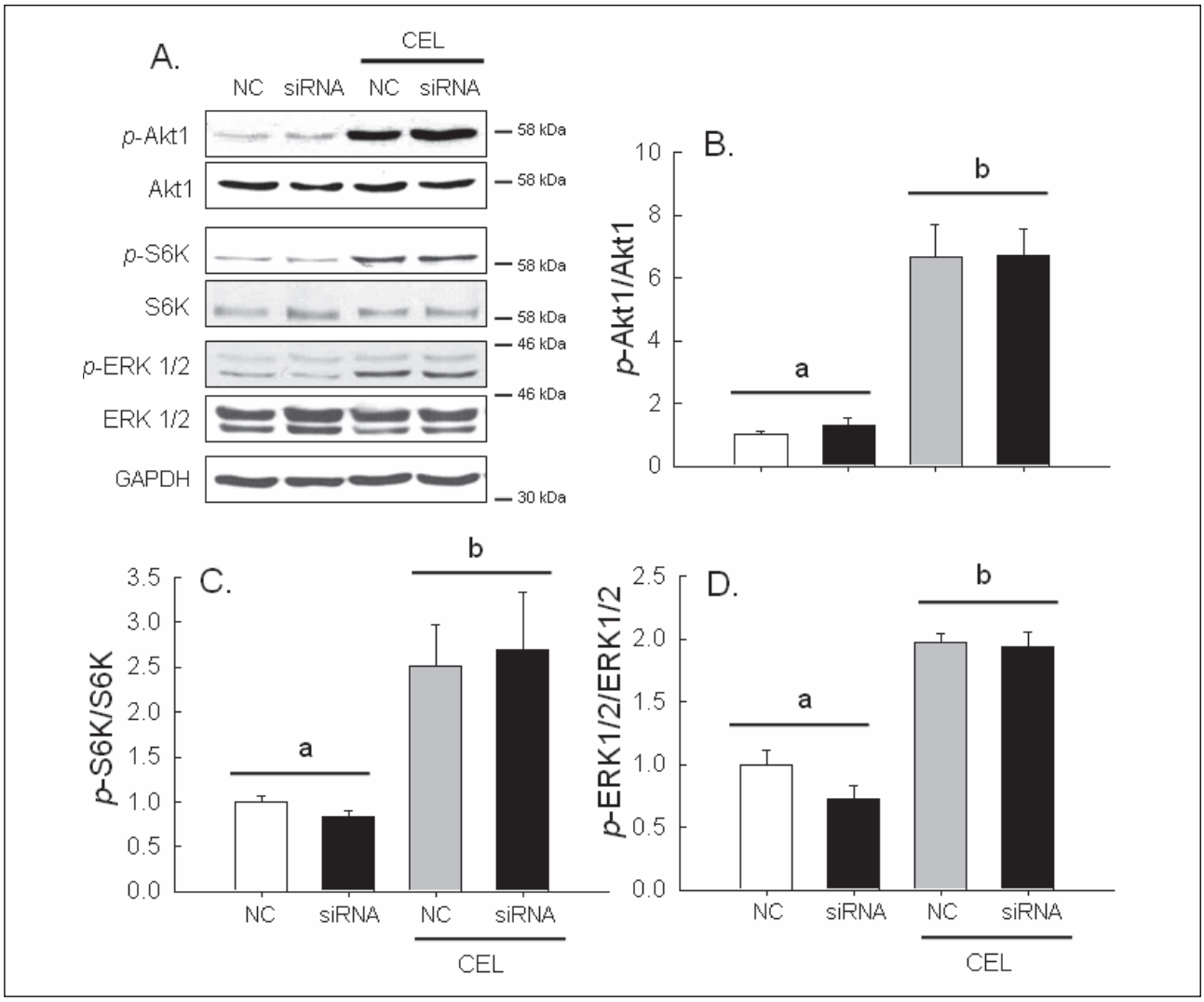

Fig. 6. Intergroup comparisons of anabolic signaling activities of Akt1, S6K and ERK1/2 by HSP72 siRNA and CEL treatment. (A) Immunoblot analysis of whole cell lysates with relevant antibodies. (B-D) The ratios of phosphorylated to unphosphorylated forms of the three signaling kinases were depicted after densitometric quantitation of respective band. Mean ±S.E.M. (n=6). a versus b, $P < 0.05$.

previous study demonstrated a decrease in the FoxO3 protein expression in mouse C212 cells by CEL treatment (6). To assess the effect of *HSP72* gene silencing on FoxO3 protein expression and phosphorylation, whole cell lysates were analyzed by immunoblotting. Compared to the NC level, phosphorylation of FoxO3 (at Ser253) was decreased 30% in the siRNA group but increased 2.4-fold in two CEL-treated groups ($P < 0.05$) (*Fig. 4A* and *4B*). In contrast, FoxO3 expression increased 1.9-fold in the siRNA group but decreased 56% the in NC + CEL group ($P < 0.05$), while the level was similar to that of the NC in the siRNA + CEL group ($P > 0.05$). As a result, the *p*-FoxO3/FoxO3 ratio decreased 60% in the siRNA group ($P < 0.05$) but was elevated 4.1-fold in the NC + CEL group ($P < 0.05$), and remained similar to the NC group in the siRNA + CEL group (*Fig. 4A* and *4D*).

Our confocal imaging also illustrated that FoxO3 expression was more abundant in the nuclei of the *HSP72* siRNA-treated cells, whereas such nuclear localization of FoxO3 was almost completely inhibited by CEL treatment (*Fig. 4E*). Furthermore, the subcellular fractionation analysis, confirmed by laminB and β-tubulin expression, demonstrated that the *p*-FoxO protein was detected only in the cytoplasm, with the protein level increased considerably by CEL treatment (*Fig. 4F*). In contrast, the FoxO3 protein expression was elevated by *HSP72* gene silencing both in the cytoplasm and in the nucleus. This *HSP72* siRNA-induced elevation, however, was ameliorated in the nucleus by CEL treatment.

HSP72 siRNA augmented atrogin-1 expression and proteasome activity that were counteracted by celastrol

To examine the effect of *HSP72* gene silencing on the catabolic activities that might influence FoxO3 expression, the ubiquitin E3 ligase expression and proteasome activity were determined by immunoblot analysis and a cell-based luminescent assay, respectively (*Fig. 5*). Compared to the NC, the atrogin-1 expression was increased 2.4-fold in the siRNA group and decreased 40% in the NC + CEL group ($P < 0.05$), while expression remained at the NC level in the siRNA + CEL group ($P > 0.05$) (*Fig. 5A* and *5B*). In contrast, MuRF1 expression was not significantly affected by siRNA, CEL, or combined treatments (*Fig. 5A* and *5C*). Finally, the chymotrypsin-like activity of the 26S proteasome was increased 4.7-fold by *HSP72* gene silencing ($P < 0.05$) but was retained at the NC level by CEL treatment. Also, the proteasome activity was not significantly affected by CEL treatment alone (*Fig. 5D*).

HSP72 siRNA treatment does not affect anabolic signaling but celastrol upregulated the signaling

To elucidate the effect of *HSP72* gene silencing and CEL on muscle protein synthesis, major anabolic signaling protein markers were assessed by immunoblot analysis. As shown in *Fig. 6A*, the *p*-Akt1 expression was profoundly increased in the CEL-treated groups, irrespective of the siRNA treatment, while the total Akt1 level was not affected by any treatment. As a result, the *p*-Akt1/Akt1 ratio increased 6.7-fold in the two CEL-treated groups compared to the NC ($P < 0.05$) (*Fig. 6B*). Phosphorylation of S6K and ERK1/2 was elevated in the CEL-treated groups, as seen in *p*-Akt1 (*Fig. 6A*). Consequently, the *p*-S6K/S6K and *p*-ERK/ERK levels increased 2.6-fold and 2.0-fold, respectively, in the two CEL-treated groups relative to the NC ($P < 0.05$) (*Fig. 6C* and *6D*).

DISCUSSION

We and others have demonstrated that HSP70 is downregulated in various muscle wasting conditions (e.g., hindlimb unloading, denervation) and that overexpression of HSP70 contributes to hypertrophy or regrowth of muscle cells (2, 6, 14-16). To induce HSP overexpression, heat stress, HSP expression plasmids, and synthetic (e.g., 17-AAG, BGP-15) and natural compounds (CEL) have been applied to muscle cells, tissues or whole organisms (1, 6, 7, 17, 18). Recent studies have also attempted to test whether muscle atrophy can be induced in the absence of HSP70 using knockout mice. According to Yasuhara *et al.* (19), wild-type and HSF1 knockout mice showed similar magnitudes of change in the soleus muscle mass and protein contents for a 2-week hindlimb suspension. After 4 weeks of reloading, however, HSF1 knockout mice exhibited a slower re-growth of the atrophied muscle with reduced expression of HSPs (e.g., HSP25 and HSP72). According to another study (20), *HSP70* knockout mice showed a smaller cross-sectional area of the soleus muscle fibers and, following muscle injury, demonstrated a delayed inflammation response and myofiber regeneration compared to those of wild type mice. Conversely, introduction of HSP70 expression plasmids into the soleus muscle of the knockout mice promoted regeneration of myofibers as well as recovery of force capacity in the damaged muscle. Although these studies imply a key role of HSP in regulation of muscle size and function, there still remains an open question of how the lack of HSP70 can lead to muscle atrophy.

We addressed this issue by applying gene-specific siRNA for *HSP72* gene silencing and CEL treatment for HSP72 induction in rat L6 myotubes. Because muscle atrophy results from excessive protein degradation relative to protein synthesis, we assessed the effect of *HSP72* silencing on major signaling regulators associated with muscle synthesis and degradation pathways. Our data demonstrated that *HSP72* siRNA was functionally effective not only for active suppression of *HSP72* mRNA and protein expression but also for an increase in FoxO3 expression in the myotubes (*Figs. 1*, *2* and *4*). Moreover, CEL treatment remarkably augmented expression of the *HSP* mRNA and protein, even in the presence of HSP72-specific siRNA mediated gene silencing in myotubes. This HSP72 increase apparently resulted from significant nuclear accumulation and phosphorylation of HSF1 in the myotubes treated with CEL for up to 6 hours (*Figs. 1* and *2*). These results, together, suggest that the *HSP72* siRNA exerted a catabolic potential with downregulation of HSP72 and upregulation of FoxO3, whereas such catabolic potency was inhibited *via* the CEL-mediated activation of HSF1 in the myotubes. This consequence was evidenced by differences in the cell size; the siRNA treatment led to atrophy of the myotube diameter (84% of that of the NC), but the CEL treatment abolished this atrophic effect (*Fig. 3*). In our previous study, CEL-treated C2C12 myotubes showed nuclear accumulation of *p*-HSF1 and overexpression of HSP72 that abolished the atrophic effect of dexamethasone (DEX) *via* suppression of catabolic signals (6). However, in that report, because DEX did not affect HSP70 expression, we were unable to address the effect of HSP70 downregulation on the muscle cell size and the changes in the relevant signaling activities (6). With the use of *HSP72* siRNA, CEL (HSP inducer) and the rat L6 myotubes, the current study allowed us to test the critical regulatory role of HSP72 in myofiber preservation in a different muscle cell line.

The transcription factor FoxO plays a central role in the control of skeletal muscle atrophy by stimulating expression of E3 ligases (atrogin-1 and MuRF1) and thereby enhancing muscle protein degradation. The Akt pathway, on the other hand, promotes muscle growth but simultaneously blocks protein degradation by phosphorylation and export of FoxO3 from the nucleus to the cytoplasm (21-23). Importantly, recent studies revealed that the FoxO3 signaling was directly regulated by HSP70 expression because the expression was increased in the nucleus of the immobilized rat soleus muscle, while it was suppressed by injection of an HSP70 expression plasmid (7). Moreover, FoxO3 plasmid injection enhanced atrogin-1 and MuRF1 promoter activities, while *HSP70* plasmid injection suppressed them. Our present study further confirmed the significance of HSP on muscle fiber regulation and provided convincing evidence to connect the HSP70 with the FoxO3 pathway in the L6 cell. As shown in *Fig. 4*, *HSP72* siRNA treatment increased FoxO3 expression but lowered FoxO3 phosphorylation, whereas CEL treatment reversed these outcomes (*Fig. 4A-4D*). Moreover, our immunofluorescent staining and subcellular fractionation analysis revealed that the siRNA-induced upregulation of FoxO3, particularly in the nucleus, was contrasted by the CEL-mediated increase of *p*-FoxO3 exclusively in the cytoplasm, which resulted in the *p*-FoxO3/FoxO3 level balanced to the NC level by siRNA + CEL treatment. Interestingly, there might be a differential effect of CEL on the levels of FoxO3 and *p*-FoxO3 depending on the cell lines used, because CEL did not alter these levels in C2C12 myotubes (6) but elicited significant changes in the L6 cells (*Fig. 4A-4D*).

Once the HSP72-FoxO3 relationship was established, we wanted to address whether the catabolic and anabolic signaling activities are matched to this relationship. Our present study revealed that the atrophy of L6 cells caused by *HSP72* siRNA treatment was in accord with increases in atrogin-1 expression and chymotrypsin-like activity of proteasomes (*Fig. 5*). Moreover, the levels of these catabolic markers were suppressed by CEL treatment, thus reflecting the retention of the myotube diameter even under the *HSP72* silencing. The MuRF1 expression was not affected by either *HSP72* siRNA or CEL and the combined treatment. Previously, we found upregulation of MuRF1 by DEX in both mouse C2C12 (6) and rat L6 myotubes (data not shown). Other studies showed that expression of atrogin-1 was regulated by activation of the FoxO family, whereas MuRF1 expression was regulated by both FoxO and NF-κB (24). These studies suggest that the E3 ligases might be differentially regulated by different transcription factors, which would be clarified in the future studies.

The activation of the Akt1-S6K and ERK1/2 pathways has been reported to promote muscle hypertrophy and cell survival *via* inhibition of FoxO transcription activity (21, 25, 26). Our results show that activation of these anabolic signals was significantly upregulated by HSP72 overexpression, while it was not affected by HSP72 silencing (*Fig. 6*). Similar results were observed in our previous experiments with DEX- and CEL-treated C2C12 myotubes (6). In our previous report, we found,

for the first time, that the Akt1 and ERK1/2 pathways were likely to be inter-linked under the CEL influence since either of the pathways could be activated when the other was inhibited. In addition, as shown in *Figs. 4* and *6* of the current study, because siRNA treatment suppressed FoxO3 phosphorylation but did not affect Akt1 and ERK1/2 activation, there appears to be a direct linkage of HSP70 to FoxO3 signaling that might be a novel regulatory mechanism for myofiber size determination.

Finally, it is also important to note that the HSR *via* HSP is ubiquitous and provides benefits in diverse *in vivo* and *in vitro* processes. Cytoprotection is the primary benefit of the HSP upregulation under various stresses, such as exercise-induced thermal stress (27), exposure to ultraviolet radiation (28) and pathogenic infection (29, 30). For instance, immune cells (e.g., monocytes) infected with bacterial pathogen elevated the nuclear translocation of HSF1 and activation of HSP70 gene transcription, which seemed to provide the defending mechanism to protect the monocytes against the toxic products of engulfed bacteria and premature apoptosis. Thus, in addition to its anti-atrophy effect in the skeletal muscle cell, the HSP induction plays a pivotal protective role in the inflammatory process of the gut smooth muscles (29).

In conclusion, our data sufficiently supported the anabolic role of HSP72 for myofiber size preservation which was regulated *via* both upregulation of FoxO3 phosphorylation and activation of Akt1-ERK1/2 signaling pathway. It is worth assessing the pro-anabolic and anti-catabolic function of CEL using an animal model to apply our *in vitro* results to a muscle-specific and a systemic function.

Acknowledgements: We would like to thank collaborators of Korea Aerospace Research Institute (KARI) and Japan Aerospace Exploration Agency (JAXA) for many detailed discussions and technical supports. We are also grateful to three anonymous reviewers for their special concerns and comments to improve the manuscript. This research was supported by the research grant "Fundamental Study of Manned Space Technology for Microgravity Environment Utilization" funded by KARI (FR13350W01).

Conflict of interest : None declared.

REFERENCES

1. Lomonosova YN, Shenkman BS, Nemirovskaya TL. Attenuation of unloading-induced rat soleus atrophy with the heat-shock protein inducer 17-(allylamino)-17-demethoxygeldanamycin. *FASEB J* 2012; 26: 4295-42301.
2. Senf SM, Dodd SL, McClung JM, Judge AR. Hsp70 overexpression inhibits NF-kappaB and Foxo3a transcriptional activities and prevents skeletal muscle atrophy. *FASEB J* 2008; 22: 3836-3845.
3. Kayama M, Nakazawa T, Thanos A, *et al.* Heat shock protein 70 (HSP70) is critical for the photoreceptor stress response after retinal detachment via modulating anti-apoptotic Akt kinase. *Am J Pathol* 2011; 178: 1080-1091.
4. Lunova M, Zizer E, Kucukoglu O, *et al.* Hsp72 overexpression accelerates the recovery from caerulein-induced pancreatitis. *PLoS One* 2012; 7: e39972.
5. Mao H, Li Z, Zhou Y, *et al.* HSP72 attenuates renal tubular cell apoptosis and interstitial fibrosis in obstructive nephropathy. *Am J Physiol Renal Physiol* 2008; 295: F202-F214.
6. Gwag T, Park K, Kim E, *et al.* Inhibition of C2C12 myotube atrophy by a novel HSP70 inducer, celastrol, via activation of Akt1 and ERK1/2 pathways. *Arch Biochem Biophys* 2013; 537: 21-30.
7. Senf SM, Dodd SL, Judge AR. FOXO signaling is required for disuse muscle atrophy and is directly regulated by Hsp70. *Am J Physiol Cell Physiol* 2010; 298: C38-C45.
8. Akerfelt M, Morimoto RI, Sistonen L. Heat shock factors: integrators of cell stress, development and lifespan. *Nat Rev Mol Cell Biol* 2010; 11: 545-555.
9. Trott A, West JD, Klaic L, *et al.* Activation of heat shock and antioxidant responses by the natural product celastrol: transcriptional signatures of a thiol-targeted molecule. *Mol Biol Cell* 2008; 19: 1104-12.
10. Holmberg CI, Hietakangas V, Mikhailov A, *et al.* Phosphorylation of serine 230 promotes inducible transcriptional activity of heat shock factor 1. *EMBO J* 2001; 20: 3800-3810.
11. Liebelt B, Papapetrou P, Ali A, *et al.* Exercise preconditioning reduces neuronal apoptosis in stroke by up-regulating heat shock protein-70 (heat shock protein-72) and extracellular-signal-regulated-kinase 1/2. *Neuroscience* 2010; 166: 1091-1100.
12. Walcott SE, Heikkila JJ. Celastrol can inhibit proteasome activity and upregulate the expression of heat shock protein genes, hsp30 and hsp70, in Xenopus laevis A6 cells. *Comp Biochem Physiol A Mol Integr Physiol* 2010; 156: 285-293.
13. Westerheide SD, Bosman JD, Mbadugha BN, *et al.* Celastrols as inducers of the heat shock response and cytoprotection. *J Biol Chem* 2004; 279: 56053-56060.
14. Gwag T, Lee K, Ju H, Shin H, Lee JW, Choi I. Stress and signaling responses of rat skeletal muscle to brief endurance exercise during hindlimb unloading: a catch-up process for atrophied muscle. *Cell Physiol Biochem* 2009; 24: 537-546.
15. Kukreti H, Amuthavalli K, Harikumar A, *et al.* Muscle-specific microRNA1 (miR1) targets heat shock protein 70 (HSP70) during dexamethasone-mediated atrophy. *J Biol Chem* 2013; 288: 6663-6678.
16. Siu PM, Pistilli EE, Murlasits Z, Alway SE. Hindlimb unloading increases muscle content of cytosolic but not nuclear Id2 and p53 proteins in young adult and aged rats. *J Appl Physiol* 2006; 100: 907-916.
17. Gehrig SM, van der Poel C, Sayer TA, *et al.* Hsp72 preserves muscle function and slows progression of severe muscular dystrophy. *Nature* 2012; 484: 394-398.
18. Naito H, Powers SK, Demirel HA, Sugiura T, Dodd SL, Aoki J. Heat stress attenuates skeletal muscle atrophy in hindlimb-unweighted rats. *J Appl Physiol* 2000; 88: 359-363.
19. Yasuhara K, Ohno Y, Kojima A, *et al.* Absence of heat shock transcription factor 1 retards the regrowth of atrophied soleus muscle in mice. *J Appl Physiol* 2011; 111: 1142-1149.
20. Senf SM, Howard TM, Ahn B, Ferreira LF, Judge AR. Loss of the inducible Hsp70 delays the inflammatory response to skeletal muscle injury and severely impairs muscle regeneration. *PLoS One* 2013; 8: e62687.
21. Brunet A, Bonni A, Zigmond MJ, *et al.* Akt promotes cell survival by phosphorylating and inhibiting a Forkhead transcription factor. *Cell* 1999; 96: 857-868.
22. Pang X, Yi Z, Zhang J, Lu B, *et al.* Celastrol suppresses angiogenesis-mediated tumor growth through inhibition of AKT/mammalian target of rapamycin pathway. *Cancer Res* 2010; 70: 1951-1959.
23. Waddell DS, Baehr LM, van den Brandt J, *et al.* The glucocorticoid receptor and FOXO1 synergistically activate the skeletal muscle atrophy-associated MuRF1 gene. *Am J Physiol Endocrinol Metab* 2008; 295: E785-E797.
24. Cai D, Frantz JD, Tawa NE, Jr., *et al.* IKKbeta/NF-kappaB activation causes severe muscle wasting in mice. *Cell* 2004; 119: 285-298.
25. Rommel C, Bodine SC, Clarke BA, *et al.* Mediation of IGF-1-induced skeletal myotube hypertrophy by

PI(3)K/Akt/mTOR and PI(3)K/Akt/GSK3 pathways. *Nat Cell Biol* 2001; 3: 1009-1013.
26. Tian T, Zhao Y, Nakajima S, *et al.* Cytoprotective roles of ERK and Akt in endoplasmic reticulum stress triggered by subtilase cytotoxin. *Biochem Biophys Res Commun* 2011; 410: 852-858.
27. Sadowska-Krepa E, Klapcinska B, Jagsz S, *et al.* Diverging oxidative damage and heat shock protein 72 responses to endurance training and chronic testosterone propionate treatment in three striated muscle types of adolescent male rats. *J Physiol Pharmacol* 2013; 64: 639-647.
28. Matsuda M, Hoshino T, Yamashita Y, *et al.* Prevention of UVB radiation-induced epidermal damage by expression of heat shock protein 70. *J Biol Chem* 2010; 285: 5848-5858.
29. Krzysiek-Maczka G, Targosz A, Ptak-Belowska A, *et al.* Molecular alterations in fibroblasts exposed to Helicobacter pylori: a missing link in bacterial inflammation progressing into gastric carcinogenesis? *J Physiol Pharmacol* 2013; 64: 77-87.
30. Pierzchalski P, Jastrzebska M, Link-Lenczowski P, *et al.* The dynamics of heat shock system activation in monomac-6 cells upon Helicobacter pylori infection. *J Physiol Pharmacol* 2014; 65: 791-800.

Received: August 24, 2014
Accepted: February 17, 2015

Author's address: Prof. Inho Choi, Division of Biological Science and Technology, Yonsei University, 1 Yonseidaegil, Wonju, Gangwon-do 220-710, Republic of Korea.
E-mail: ichoi@yonsei.ac.kr